

Research Article

Lakshmi Sireesha Challa, Ravi Ragoju, Sathishkumar Veerappampalayam Easwaramoorthy, and Jaehyuk Cho*

Linear instability of the vertical throughflow in a porous layer saturated by a power-law fluid with variable gravity effect

<https://doi.org/10.1515/phys-2024-0049>
received November 24, 2023; accepted June 05, 2024

Abstract: The present study investigates the thermal convection of a power-law fluid in a horizontal porous layer that is heated from below. The study of flow in a porous medium is important because of its applications in various fields such as agriculture, geothermal sciences, and engineering. Linear instability analysis is performed using the normal mode method to solve the governing equations after non-dimensionalization. The bvp4c routine in MATLAB R2020a has been used to solve the raised problem for linear instability. The impact of gravity parameter, Peclet number, and power-law index on linear instability has been investigated. Linear and quadratic variations of gravity field are considered. From the results, it is evident that the critical Rayleigh number exhibits a non-monotonic relationship with the Peclet number. Increasing the gravity variation parameter leads to a more stable system, particularly in the case of linear gravity variation.

Keywords: linear stability, porous media, power-law fluid, variable gravity

Nomenclature

d	length (m)
k	thermal diffusivity (m^2/s)
K	permeability (H/m)
T	temperature (K)
t	time (s)
P	pressure (N/m^2)
g	acceleration due to gravity (m/s^2)
\bar{u}	fluid velocity (m/s)
$\bar{u}, \bar{v}, \bar{w}$	velocity components
w_0	prescribed vertical throughflow velocity
Dimensionless parameters	
n	power-law index
Pe	Peclet number
q	wave number
Ra	Rayleigh number
Greek symbols	
β	thermal expansion coefficient ($(\text{m/m})/\text{ }^\circ\text{C}$)
σ	ratio of heat capacitance
μ	consistency factor
ϕ	porosity (mL/min)
ρ	fluid density (kg/m^3)
χ	thermal diffusivity (m^2/s)
δ	gravity parameter

* Corresponding author: Jaehyuk Cho, Department of Software Engineering and Division of Electronics and Information Engineering, Jeonbuk National University, Jeonju-si, 54896, Republic of Korea, e-mail: chojh@jbnu.ac.kr

Lakshmi Sireesha Challa: Department of Mathematics, CBIT Hyderabad, Hyderabad, India

Ravi Ragoju: Department of Applied Sciences, National Institute of Technology Goa, Goa, India

Sathishkumar Veerappampalayam Easwaramoorthy: Department of Computing and Information Systems, Sunway University, 47500, Petaling Jaya, Selangor Darul Ehsan, Malaysia

1 Introduction

Throughflow is a type of irregular horizontal internal water flow within the soil mantle, which occurs when the soil is fully saturated due to high precipitation. Understanding the onset of convective phenomena and throughflow influence in porous domains holds significant importance in various geophysical applications within the Earth and in technical

applications such as railroad constructions, frozen soil conditions, road freezing, and frost heave [1–3]. Neglecting viscous dissipation as well as inertial impacts and based on Darcy model, Nield and Kuznetsov [4] discussed the through-flow on convective phenomena in horizontal porous layers. Deepika and Narayana [5] analyzed the impacts of vertical through flow and variable gravity field using energy functional. Shooting as well as Runge–Kutta methods are employed for solving eigen value problem at both effects and observed that linear stability results lead to overprediction of onset of convection. Kiran [6] studied the vertical throughflow and periodic gravitation effects on Darcy convection. Throughflow helps in stabilization and destabilization of the system for isothermal as well as stress-free boundary conditions. Yadav *et al.* [7] examined linear, parabolic, and exponential types of gravitational forces on the formation of nanofluid convective instability and proved that the throughflow and gravity inconsistency interrupt the onset of convective instability.

In the study of the behavior of materials in fluid mechanics, including mud, clay, honey, slurries, blood, hair, ink, chocolates, gel, and paints, a power-law fluid is often used as an idealized fluid model. In this model, the shear stress is considered a function of the shear rate at a particular time. The constitutive relation for such fluids is a generalized form of the power-law fluid model [8–10]. It satisfies the analysis of flow of matter and primarily in state equations. Tsakiroglou [11] presented analytic models to address the generalized Newtonian fluid movement in porous domain. Lattice Boltzmann approach is employed by Sullivan *et al.* [12] for flow analysis of power-law fluid in a complex porous domain at the pore scale in two and three dimensions. Pascal [13] investigated the structure and generation of roll waves growing on the surface of a power-law fluid flowing down an inclined porous domain. The extension of classical Prats problem was given by Barletta and Nield [14] for special case of Newtonian and power-law fluids. They observed that the Pecllet number value over basic flow significantly influences the Darcy–Rayleigh as well as critical wave numbers. For power-law fluid, the Prats problem is generalized with the Horton–Rogers–Lapwood problem and is observed to be linearly stable. Generalization of linear instability during vertical throughflow effect of a power-law fluid in a porous domain containing permeable as well as isothermal boundaries was the main focus of Barletta and Storesletten [15]. Taking the impacts of internal heating as well as viscous dissipation into consideration, Kumari and Murthy [16] observed the throughflow effect in a horizontal porous domain containing power-law fluid and by considering the third type of boundary heating constraints. Later, Celli *et al.* [17] examined throughflow in a power-law fluid drenched porous horizontal domain with the impact of an open boundary. Variable gravity models

and the strength of gravity are measured with the Planck mass, which bank on the value of a scalar field and the cosmological parameters. In this system, porous medium drenched by a power-law fluid is considered to analyze the gravity variation impact on the onset of convective phenomena. Further details on convective phenomena in power-law fluid can be found in the study by Reddy *et al.* [18–20].

Considering a variable gravity field, Straughan [21] studied the onset of convection, while Alex and Patil [22,23] identified results of Soret and driven effects in internal heat source and inclined anisotropic porous domain. Harfash [24] analyzed a three-dimensional porous domain by the consideration of gravity variation along with internal heat source. Yadav [25] considered the variable gravity effect to study the convective instabilities of a fluid flow.

The literature lacks investigations on the impact of gravity variation on the onset of convection of a power-law fluid in a porous layer. In this study, we explore the onset of convection of a power-law fluid in a porous layer considering throughflow and variable gravity effects. Through linear theory and normal mode analysis, we examine the implications. This research holds potential application in assessing solar pond performance, where a porous medium stabilizes the system. The downward flow facilitates the transfer of absorbed solar radiation through the water-saturated porous medium to the pond bottom, maintaining warm water for practical use with minimal downward velocities. The article is structured as follows: Section 2 provides a brief overview of the mathematical formulation of the problem. In Section 3, the normal mode approach is utilized to solve the dimensionless governing equations, facilitating linear stability analysis. The study concludes with discussion and conclusion in Section 4 and 5, respectively.

2 Mathematical formulation

A porous, homogeneous, isotropic horizontal plane having thickness d , logged by a power-law fluid with variable gravity $\bar{g}(z)$ is considered in the current investigation. Darcy's law along with Oberbeck–Boussinesq approximation is employed to analyze the power-law type of non-Newtonian fluid behavior. The governing equations of the considered mathematical model are given as follows [15,18,21]:

$$\nabla \cdot \mathbf{u} = 0, \quad (2.1)$$

$$\frac{\mu^*}{K} |\mathbf{u}|^{n-1} \mathbf{u} = -\nabla P - \rho_0 \bar{g}(z) + \beta(T - T_0) \hat{e}_z, \quad (2.2)$$

$$\sigma \frac{\partial T}{\partial t} + (\mathbf{u} \cdot \nabla) T = \chi \nabla^2 T, \quad (2.3)$$

based on the boundary conditions

$$\begin{aligned} w &= w_0, T = T_0 + \Delta T \quad \text{on} \quad z = 0, \\ w &= w_0, T = T_0 \quad \text{on} \quad z = 1. \end{aligned} \quad (2.4)$$

Considering the Newtonian case, then $n = 1$ and $\frac{\mu^*}{K} = \frac{\mu}{K}$,

$$\mu^*/K = 2\xi\mu\left(\frac{3}{50}\frac{\phi}{K}\right)^{\frac{n+1}{2}}\left(\frac{1+3n}{n\phi}\right)^n, \quad (2.5)$$

subject to variable gravity $\bar{g}(z) = g_0[1 + \delta G(z)]$, reference gravity is g_0 , $G(z)$ denotes functional gravity variation values, δ indicates the parameter for gravity variation and the tortuosity is $\xi = 25/12$, which was given by Christopher and Middleman [26]. The following non-dimensional variables are introduced:

$$\begin{aligned} x &= x^*d, \quad y = y^*d, \quad z = z^*d, \\ u &= \frac{\chi}{d}u^*, \quad v = \frac{\chi}{d}v^*, \quad w = \frac{\chi}{d}w^*, \\ t &= \frac{\sigma d^2}{\chi}t^*, \quad T = T_0T^*, \end{aligned} \quad (2.6)$$

which are subject to the dimensionless parameter Rayleigh number Ra for power-law fluid and Peclet number Pe

$$\text{Ra} = \frac{g_0\rho_0\beta\Delta TKd^n}{\chi^n\mu} \quad \text{Pe} = \frac{w_0d}{\phi}. \quad (2.7)$$

Eqs (2.1)–(2.3) in dimensionless form, curl of Eq. (2.2) and boundary conditions in non-dimensional form (2.4) are given as:

$$\nabla \cdot \mathbf{u} = 0, \quad (2.8)$$

$$\nabla \times (|\mathbf{u}|^{n-1}\mathbf{u}) = [1 + \delta G(z)]\text{Ra}\nabla \times (T\hat{e}_z), \quad (2.9)$$

$$\frac{\partial T}{\partial t} + (\mathbf{u} \cdot \nabla)T = \nabla^2 T, \quad (2.10)$$

$$w = \text{Pe}, \quad T = 1 \quad \text{on} \quad z = 0, \quad (2.11)$$

$$w = \text{Pe}, \quad T = 0 \quad \text{on} \quad z = 1.$$

2.1 Basic state

The uniform basic throughflows of Eqs (2.8)–(2.11) are given by

$$u_b = v_b = 0, \quad w_b = \text{Pe}. \quad (2.12)$$

The basic state is denoted by subscript b and Peclet number is represented by Pe. The basic temperature profile is obtained by substituting Eq. (2.12) in Eq. (2.10), namely,

$$T_b = \frac{e^{\text{Pe}} - e^{\text{Pe}z}}{e^{\text{Pe}} - 1}. \quad (2.13)$$

3 Linear stability analysis

Basic state Eqs (2.8)–(2.11) are perturbed as

$$\mathbf{u} = \mathbf{u}_b + \varepsilon\mathbf{u}', T = T_b + \varepsilon T', \quad (3.1)$$

where $\varepsilon \ll 1$. Substituting Eq. (3.1) in Eqs (2.8)–(2.11) and ignoring higher order terms $O(\varepsilon^2)$ give:

$$\frac{\partial u'}{\partial x} + \frac{\partial v'}{\partial y} + \frac{\partial w'}{\partial z} = 0, \quad (3.2)$$

$$|\text{Pe}|^{n-1}\left[n\frac{\partial w'}{\partial y} - \frac{\partial v'}{\partial z}\right] = \text{Ra}[1 + \delta G(z)]\frac{\partial T'}{\partial y}, \quad (3.3)$$

$$|\text{Pe}|^{n-1}\left[n\frac{\partial w'}{\partial x} - \frac{\partial u'}{\partial z}\right] = \text{Ra}[1 + \delta G(z)]\frac{\partial T'}{\partial x}, \quad (3.4)$$

$$\frac{\partial u'}{\partial y} - \frac{\partial v'}{\partial x} = 0, \quad (3.5)$$

$$\frac{\partial T'}{\partial t} + w'\frac{dT_b}{dz} + \text{Pe}\frac{\partial T'}{\partial z} = \nabla^2 T', \quad (3.6)$$

$$w' = 0, \quad T' = 0, \quad z = 0, 1, \quad (3.7)$$

where $\nabla^2 = \frac{\partial^2}{\partial x^2} + \frac{\partial^2}{\partial y^2} + \frac{\partial^2}{\partial z^2}$ and simplifying Eqs (3.2)–(3.7), we obtain

$$\begin{aligned} n\left(\frac{\partial^2 w'}{\partial x^2} + \frac{\partial^2 w'}{\partial y^2}\right) + \frac{\partial^2 w'}{\partial z^2} \\ = \frac{\text{Ra}}{|\text{Pe}|^{n-1}}[1 + \delta G(z)]\left(\frac{\partial^2 T'}{\partial x^2} + \frac{\partial^2 T'}{\partial y^2}\right), \end{aligned} \quad (3.8)$$

$$\frac{\partial T'}{\partial t} + \frac{dT_b}{dz}w' + \text{Pe}\frac{\partial T'}{\partial z} - \nabla^2 T' = 0, \quad (3.9)$$

$$w' = 0, \quad T' = 0, \quad z = 0, 1. \quad (3.10)$$

We used normal mode technique for this system, it is in the form of

$$(w', T') = [W(z), \theta(z)]e^{i(mx+ly-\omega t)}, \quad (3.11)$$

where resulting dimensionless wave number is $q = \sqrt{l^2 + m^2}$, negative x and y direction wave numbers are m and l , and growth rate of instability is ω . On putting Eq. (3.11) into Eqs (3.8)–(3.10), they become

$$(D^2 - nq^2)W + \frac{\text{Ra}}{|\text{Pe}|^{n-1}}[1 + \delta G(z)]q^2\theta = 0, \quad (3.12)$$

$$[(D^2 - \text{Pe}D - q^2 - i\omega)\theta + \text{Pe}F(z)]W = 0, \quad (3.13)$$

$$\theta = W = 0, \quad z = 0, 1, \quad (3.14)$$

where $F(z) = \frac{e^{\text{Pe}z}}{e^{\text{Pe}} - 1}$ and $G(z)$ is referred from Rionero and Straughan [27] and taken as $G(z) = -z$ and $-z^2$. Assuming the principle of exchange of stabilities, we further consider $\omega = 0$. Then, Eqs (3.12)–(3.14) are

Table 1: For Newtonian fluid, comparison of the current results with that of Barletta *et al.* [29] (for Gebhart number $Ge = 0$) for case $\delta = 0$

Pe	Barletta <i>et al.</i> [29]	Current study	Pe	Barletta <i>et al.</i> [29]	Current study
-0.001	39.4784	39.478419	0.001	39.4784	39.478419
-0.01	39.4786	39.478557	0.01	39.4786	39.478557
-0.1	39.4924	39.492367	0.1	39.4924	39.492367
-1	40.8751	40.875071	1	40.8751	40.875071
-2	45.0776	45.077609	2	45.0776	45.077609
-3	52.0684	52.068416	3	52.0684	52.068416
-4	61.6664	61.666416	4	61.6664	61.666416
-5	73.4146	73.414558	5	73.4146	73.414558
-6	86.6192	86.619201	6	86.6192	86.619201
-7	100.581	100.580850	7	100.581	100.580851
-8	114.833	114.832604	8	114.833	114.832604
-9	129.167	129.166853	9	129.167	129.166852
-10	143.518	143.518491	10	143.518	143.518491
-15	215.283	215.282801	15	215.283	215.282799

$$(D^2 - nq^2)W + \frac{Ra}{|Pe|^{n-1}}[1 + \delta G(z)]q^2\theta = 0, \quad (3.15)$$

$$[(D^2 - PeD - q^2)\theta + PeF(z)]W = 0, \quad (3.16)$$

$$\theta = W = 0, \quad z = 0, 1. \quad (3.17)$$

4 Discussion of results

This section elucidates the discussion of the numerical observations. The present analysis investigates the thermal convection of a power-law fluid in a horizontal porous layer that is heated from below. To the best of our knowledge, this study has not been reported so far. We consider the upward throughflow ($Pe > 0$). In addition to linear stability analysis approach, the dimensional basic equations are solved by employing the normal mode method. The

linear and nonlinear instabilities of the eigenvalue problem employed with the bvp4c routine in MATLAB R2020a are presented. For a detailed knowledge of the numerical methods, one can refer to the study by Reddy and Ravi [28]. Linear and quadratic variations of gravity field at $G(z) = -z$ and $G(z) = -z^2$ are investigated, respectively. The impact of gravity parameter, Peclet number, and power-law index on linear instability has been investigated. The critical Rayleigh number (Ra_c) is calculated for different prescribed value of other parameters and shown graphically.

Our numerical observations are validated in comparison with the existing results of Barletta *et al.* [29] taking $\delta = 0$. Convective roll instabilities were investigated by Barletta *et al.* in a horizontal porous layer due to throughflow with viscous dissipation. The numerical results obtained in the current investigation are in good agreement with the findings of Barletta *et al.* [29] (Table 1).

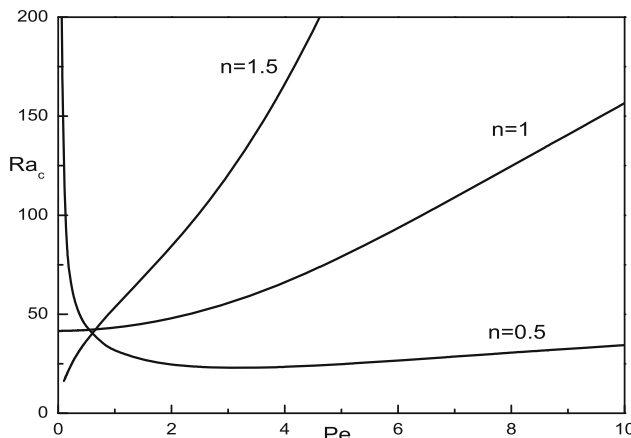


Figure 1: Critical Rayleigh number variation with Pe for $\delta = 0.1$ and $G(z) = -z$.

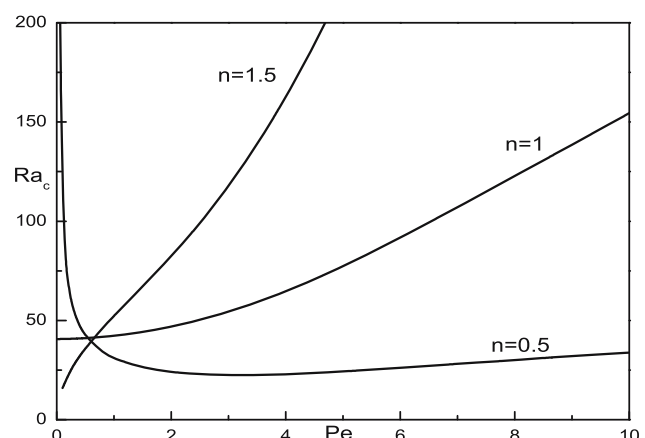


Figure 2: Critical Rayleigh number variation with Pe for $\delta = 0.1$ and $G(z) = -z^2$.

Table 2: Variation in critical Ra with δ for $Pe = 5$ and $n = 0.5$

δ	$G(z) = -z$		$G(z) = -z^2$	
	Critical Ra	Critical q	Critical Ra	Critical q
0.2	26.77551721	4.871084337	25.63904325	4.871084337
0.4	31.89371751	4.791566265	28.83363661	4.791566265
0.6	39.32931882	4.672289157	32.85387105	4.672289156
0.8	50.97951944	4.553012048	38.02461168	4.553012048

Table 3: Variation in critical Ra with δ for $Pe = 5$ and $n = 1$

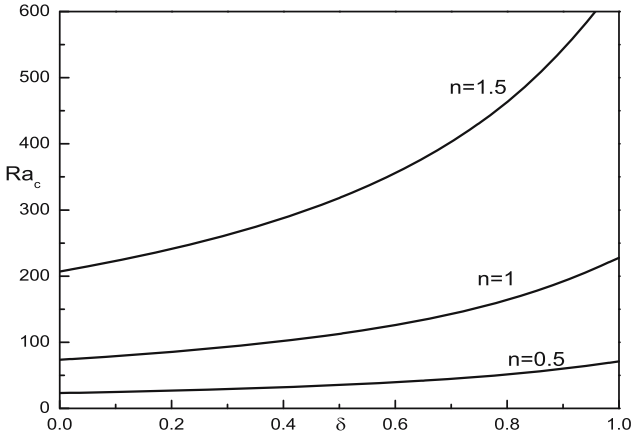
δ	$G(z) = -z$		$G(z) = -z^2$	
	Critical Ra	Critical q	Critical Ra	Critical q
0.2	85.31614717	4.1554216	81.701916957	4.115662656
0.4	101.6843525	4.0759036	91.938936926	4.791566265
0.6	125.4839766	3.9566265	104.83077354	3.956626506
0.8	162.8095520	3.8373493	121.420318003	3.837349397

Figures 1 and 2 illustrate the change in critical Rayleigh number for various minimal Peclet number values, with variation in n . From the figure, it is evident that at low Peclet numbers, Ra_c initially decreases before increasing for $n < 1$. However, for $n \geq 1$, it consistently increases. In the case of shear-thinning fluids, Ra_c exhibits a non-monotonic relationship with Pe , while for shear-thickening and Newtonian fluids, Ra_c behaves as a monotonic function of Pe . The apparent viscosity of pseudoplastic fluids tends toward infinity as the shear rate approaches zero (i.e., for small Pe), whereas it tends toward zero for dilatant fluids at low shear rates. Higher values of Ra_c indicate inhibition of convective instability for pseudoplastic fluids, whereas clear instability is indicated by diminishing values of Ra_c for dilatant fluids under fixed parameter values. Additionally, Ra_c gradually increases for large Peclet numbers.

The graphical results in Figures 3 and 4 illustrate the change in critical Ra as a function of δ (gravity variation

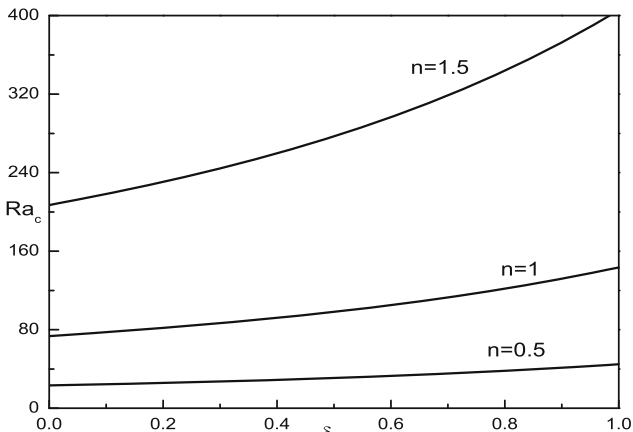
Table 4: Variation in critical Ra with δ for $Pe = 5$ and $n = 1.5$

δ	$G(z) = -z$		$G(z) = -z^2$	
	Critical Ra	Critical q	Critical Ra	Critical q
0.2	240.5441101	3.75783132	230.3799816	3.75783132
0.4	286.8854341	3.67831325	259.4277647	3.67831325
0.6	354.3399074	3.59879518	296.0457215	3.59879518
0.8	460.2905691	3.47951807	343.2103923	3.47951807

**Figure 3:** Critical Rayleigh number variation with δ for $Pe = 5$ and $G(z) = -z$.

parameter) for cases where $G(z) = -z$ and $G(z) = -z^2$, respectively. It is evident from these graphs that as δ increases, the critical Ra enhances, and the gravity variation parameter has a stabilizing effect on the system, resulting in a deterioration of the gravity field due to an increase in δ value. An increase in δ value leads to a decline in the gravity field. The frustration in the system diminishes as the gravity field reduces, postponing the onset of convection.

Tables 2–4 exhibit an increasing trend of critical Ra with δ , consistent with the observations from Figures 3 and 4. For the case $G(z) = -z$, the critical Ra exceeds that of the case $G(z) = -z^2$. In other words, the system demonstrates greater stability under linear gravity variation compared to parabolic variation. Moreover, critical q is a decreasing function of δ for all cases.

**Figure 4:** Critical Rayleigh number variation with δ for $Pe = 5$ and $G(z) = -z^2$.

5 Conclusion

The study investigates thermal convection of a power-law fluid in a porous layer heated from below, employing linear instability analysis. Critical Rayleigh numbers are computed for linear theory, and the instability analysis is numerically conducted using the bvp4c solver in MATLAB R2020a. The obtained results align well with those available in the literature for limiting cases. Depending on the Peclet number, the critical Rayleigh number exhibits either a monotonic increasing or decreasing trend relative to the power-law index. The gravity parameter stabilizes the system for all values of n , with enhanced stability observed in cases of linear gravity variation. This study bears significant applications in industrial and geophysical engineering. In the future, we aim to extend the analysis to include transverse rolls by exploring additional variations in the gravity parameter.

Funding information: This work was supported by the Korea Environmental Industry and Technology Institute (KEITI), with a grant funded by the Korean Government, Ministry of Science and Environment (The development of IoT-based technology for collecting and managing big data on environmental hazards and health effects), under grant RE202101551.

Author contributions: Lakshmi Sireesha Challa: conceptualizations, methodology, software, writing, and editing; Ravi Ragoju: conceptualizations, methodology, writing, and editing; Sathishkumar Veerappampalayam Easwaramoorthy: software, writing and editing; and Jaehyuk Cho: software, writing and editing. All authors have accepted responsibility for the entire content of this manuscript and approved its submission.

Conflict of interest: The authors state no conflict of interest.

References

- [1] Prakash D, Muthamil Selvan M, Doh DH. Effect of heat generation on forced convection through a porous saturated duct. *Transport Porous Media*. 2012;95:377–88.
- [2] Prakash D, Suriyakumar P, Sivakumar N, Kumar BR. Influence of viscous and Ohmic heating on MHD flow of nanofluid over an inclined nonlinear stretching sheet embedded in a porous medium. *Int J Mechanic Eng Technol.* 2018;9(8):992–1001.
- [3] Ragupathi E, Prakash D, Muthamil Selvan M, Al-Mdallal QM. Impact of thermal nonequilibrium on flow through a rotating disk with power law index in porous media occupied by Ostwald-de-Waele nanofluid. *J Non-Equilib Thermodyn.* 2022;47(4):375–94.
- [4] Nield DA, Kuznetsov AV. The onset of convection in a layered porous medium with vertical throughflow. *Transp Porous Media*. 2013;98:363–76.
- [5] Deepika N, Narayana PAL. Effects of vertical throughflow and variable gravity on Hadley-Prats flow in a porous medium. *Transport Porous Media*. 2015;109(2):455–68.
- [6] Kiran P. Throughflow and gravity modulation effects on heat transport in a porous medium. *J Appl Fluid Mechanics*. 2016;9(3):1105–13.
- [7] Yadav D, Chu YM, Li Z. Examination of the nanofluid convective instability of vertical constant throughflow in a porous medium layer with variable gravity. *Appl Nanosci.* 2023;13:353–66.
- [8] Cui J, Munir S, Farooq U, Rabie MEA, Muhammad T, Razzaq R. On numerical thermal transport analysis of three-dimensional bio-convective nanofluid flow. *J Math.* 2021;2021:1–11.
- [9] Munir S, Maqsood A, Farooq U, Hussain M, Siddiqui MI, Muhammad T. Numerical analysis of entropy generation in the stagnation point flow of Oldroyd-B nanofluid. *Waves Random Complex Media*. 2022;1–17.
- [10] Farooq J, Mushtaq M, Munir S, Ramzan M, Chung JD, Farooq U. Slip flow through a non-uniform channel under the influence of transverse magnetic field. *Sci Rep.* 2018;8(1):13137.
- [11] Tsakiroglou CD. A methodology for the derivation of non-Darcian models for the flow of generalised Newtonian fluids in porous media. *J Non-Newt Fluid Dyn.* 2002;105:79.
- [12] Sullivan SP, Gladden LF, Johns ML. Simulation of power-law fluid flow through porous media using lattice Boltzmann techniques. *J Non-Newt Fluid Mechanics*. 2006;133(2–3):91–98.
- [13] Pascal JP. Instability of power-law fluid flow down a porous incline. *J Non-Newt Fluid Mechanics* 2006;133(2–3):109–20.
- [14] Barletta A, Nield DA. Linear instability of the horizontal throughflow in a plane porous layer saturated by a power-law fluid. *Phys Fluids*. 2011;23(1):013102.
- [15] Barletta A, Storesletten L. Linear instability of the vertical throughflow in a horizontal porous layer saturated by a power-law fluid. *Int J Heat Mass Transfer*. 2016;99:293–302.
- [16] Kumari S, Murthy PVSN. Stability of the horizontal throughflow of a power-law fluid in a double-diffusive porous layer under convective boundary conditions. *Int J Thermal Sci.* 2019;146:106098.
- [17] Celli M, Impombato AN, Barletta A. Buoyancy-driven convection in a horizontal porous layer saturated by a power-law fluid: The effect of an open boundary. *Int J Thermal Sci.* 2020;152:106302.
- [18] Reddy GSK, Ragoju R. Thermal instability of a power-law fluid saturated porous layer with an internal heat source and vertical throughflow. *Heat Transfer*. 2022;51(2):2181–200.
- [19] Reddy GSK, Ravi R, Matta A. Onset of triply diffusive convection in a power-law fluid saturated porous layer. *Meccanica*. 2022;57(9):2269–80.
- [20] Reddy GSK, Ragoju R, Reddy NK, Edla DR. Dissolution-driven convection of a power-law fluid in a porous medium in the presence of chemical reaction. *Heat Transfer*. 2023;53(1):3–15.
- [21] Straughan B. Convection in a variable gravity field. *J Math Anal Appl.* 1989;140(2):467–75.
- [22] Alex SM, Patil PR. Effect of variable gravity field on Soret driven thermosolutal convection in a porous medium. *Int Commun Heat Mass Transfer*. 2013;28(4):509–18.
- [23] Alex SM, Patil PR. Effect of a variable gravity field on convection in an anisotropic porous medium with internal heat source and inclined temperature gradient. *J Heat Transfer*. 2002;124(1):144–50.

- [24] Harfash AJ. Three-dimensional simulations for convection in a porous medium with internal heat source and variable gravity effects. *Transport Porous Media*. 2013;101(2):281–97.
- [25] Yadav D. Numerical investigation of the combined impact of variable gravity field and throughflow on the onset of convective motion in a porous medium layer. *Int Commun Heat Mass Transfer*. 2019;108:104274.
- [26] Christopher RH, Middleman S. Power-law flow through a packed tube. *Ind Eng Chem Fundam*. 1965;4(4):422–6.
- [27] Rionero S, Straughan B. Convection in a porous medium with internal heat source and variable gravity effects. *Int J Eng Sci*. 1990;28(6):497–503.
- [28] Reddy GSK, Ravi R. Thermal instability of a Maxwell fluid saturated porous layer with chemical reaction. *Special Topics Reviews Porous Media*. 2022;13:33–47.
- [29] Barletta A, Rossi di Schio E, Storesletten L. Convective roll instabilities of vertical throughflow with viscous dissipation in a horizontal porous layer. *Transp Porous Media*. 2010;81:461–77.

Appendix

The eigenvalue problem for linear instability is solved using the `bvp4c` routine in MATLAB R2020a. We transform Eqs (3.15)–(3.17) into a system of first-order ordinary differential equations. We impose the normalization condition $w'(0) = 1$ to obtain a non-zero solution of the eigenvalue pro-

blem. Utilizing this condition, we determine the eigenvalue Ra . To compute the critical Rayleigh number Ra_c and the corresponding wave number q_c , we employ the `indexmin` command in MATLAB R2020a. To achieve higher-order accuracy, we set the absolute and relative tolerance as 10^{-9} and 10^{-6} , respectively.